Journal of Medicinal Chemistry

Volume 50, Number 13 June 28, 2007

Articles

Fluorescently Labeled Analogues of Dofetilide as High-Affinity Fluorescence Polarization Ligands for the Human Ether-a-go-go-Related Gene (hERG) Channel

David H. Singleton,[†] Helen Boyd,[#] Jill V. Steidl-Nichols,[‡] Matt Deacon,[§] Marcel J. de Groot,[||] David Price,[||] David O. Nettleton,[†] Nora K. Wallace,[†] Matthew D. Troutman,[∞] Christine Williams,[#] and James G. Boyd*[,†]

Exploratory Medicinal Sciences and ADME Technology Group, Pfizer Global Research and Development, Groton, Connecticut, HTS Center of Emphasis, Primary Pharmacology Group, and Department of Medicinal Chemistry, Pfizer Global Research and Development, Sandwich, U.K., and Global Safety Pharmacology, Pfizer Global Research and Development, La Jolla, California 92037

Received January 15, 2007

Novel fluorescent derivatives of dofetilide (**1**) have been synthesized. Analogues that feature a fluorescent probe attached through an aliphatic spacer to the central tertiary nitrogen of **1** have high affinity for the hERG channel, and affinity is dependent on both linker length and pendent dye. These variables have been optimized to generate Cy3B derivative **10e**, which has hERG channel affinity equivalent to that of dofetilide. When bound to cell membranes expressing the hERG channel, **10e** shows a robust increase in fluorescence polarization (FP) signal. In a FP binding assay using **10e** as tracer ligand, K_i values for several known hERG channel blockers were measured and excellent agreement with the literature K_i values was observed over an affinity range of 2 nM to 3 μM. **10e** blocks hERG channel current in electrophysiological patch clamp experiments, and computational docking experiments predict that the dofetilide core of **10e** binds hERG channel in a conformation similar to that previously predicted for **1**. These analogues enable high-throughput hERG channel binding assays that are rapid, economical, and predictive of test compounds' potential for prolonged QT liabilities.

Introduction

The human ether-a-go-go-related gene (hERG[a]) encodes for a potassium channel that is expressed in the myocardium and whose activity is critical for repolarization of cardiac tissue during the heart beat cycle. The hERG channel is the molecular target of class III antiarrhythmic drugs,[1] and functional mutations in hERG are associated with a phenomenon known as QT prolongation (LQT), a lengthening of the interval required for ventricular repolarization during a single cardiac cycle.[2] LQT can have adverse effects on cardiac rhythm and can lead to a potentially lethal arrhythmia known as torsades de points. Since the cloning and functional assignment of hERG, it has also been

* To whom correspondence should be addressed. Address: Exploratory Medicinal Sciences, Pfizer Global Research and Development, Mail Stop 4014, Eastern Point Road, Groton, CT 06340. Phone: 860-441-1580. Fax: 860-441-3858. E-mail: james_g_boyd@pfizer.com.

[†] Exploratory Medicinal Sciences, Pfizer, CT.

[#] HTS Center of Emphasis, Pfizer, U.K.

[‡] Global Safety Pharmacology, Pfizer, CA.

[§] Primary Pharmacology Group, Pfizer, U.K.

[||] Department of Medicinal Chemistry, Pfizer, U.K.

[∞] ADME Technology Group, Pfizer, CT.

[a] Abbreviations: ACN, acetonitrile; Boc, *tert*-butyloxycarbonyl; DIEA, diisopropylethylamine; DMF, *N*,*N*-dimethylformamide; ESMS, electrospray mass spectrometry; FP, fluorescence polarization; *g*, gravity; HATU, *N*-[(dimethylamino)-1*H*-1,2,3-triazolo[4,5-*b*]pyridin-1-ylmethylene]hexafluorophosphate *N*-oxide; HBTU, 2-(1*H*-benzotriazol-1-yl)-1,1,3,3-tetramethyluronium hexafluorophosphate; HEK293, human embryonic kidney (cells); hERG, human ether-a-go-go-related gene; HILIC, hydrophilic interaction chromatography; HOAt, 1-hydroxy-7-azabenzotriazole; HPLC, high-pressure liquid chromatography; HRMS, high-resolution mass spectrometry; HT, high throughput; HTS, high-throughput screening; LQT, prolonged QT interval; MR121, 1-(3-carboxypropyl)-11-ethyl-1,2,3,4,8,9,10,11-octahydrodipyrido[3,2-*b*:2′,3′-*i*]phenoxazin-13-ium inner salt; MSA, methanesulfonanilide; NBD, 7-nitrobenzodiazole; NHS, *N*-hydroxysuccinimide; NMP, *N*-methylpyrrolidinone; ; SAR, structure−activity relationship; SPA, scintillation proximity assay; TFA, trifluoroacetic acid; TMR, tetramethylrhodamine.

10.1021/jm0700565 CCC: $37.00
Published on Web 05/31/2007

shown that a number of marketed therapeutic drugs have off-target affinity for the hERG channel, and the observation of LQT in patients using these drugs has been assigned to this activity. Several launched drugs with LQT side effects have been recalled.[3]

Appropriately, regulatory agencies now look scrupulously for evidence of QT prolongation during the drug application process. In order to avoid bringing a compound with LQT side effects to clinical trials, the pharmaceutical industry has devised an array of in vitro assays that are predictive of this effect. The electrophysiological patch clamp assay has emerged as an industry standard for measuring functional hERG channel blockage by small-molecule drug candidates or leads.[4,5] However, in its current format, the patch clamp assay is not suitable for rapid screening of large numbers of compounds.[6] Higher throughput patch clamp assays have been developed recently,[7,8] but these likely lack the capacity needed to fully support high-speed medicinal chemistry programs. Because affinity for the hERG channel correlates well with channel current blockage, drug discovery companies have developed radioligand-based hERG channel competition binding assays that are predictive, robust, and amenable to high throughput.[9−12] It is important to note that these assays reflect the binding mode of the particular tracer ligand used. Compounds that do not compete with the ligand may still block channel current but can be registered as false negatives. Conversely, ligands that do compete with the tracer but do not block the channel may be registered as false positives. Thus, ligand-based methods are not ideal surrogates for patch clamp experiments. They are used most effectively for HTS hit assessment and in medicinal chemistry lead development programs where speed and high throughput are required.

Radioligand-based high-throughput assays suffer from several undesirable burdens. These include regulatory agency documentation, radioactive waste-disposal, special safety training, and environmental monitoring. Fluorescence-based methods,[13] particularly fluorescence polarization (FP) methods, have emerged as versatile screening alternatives with greatly reduced environmental and cost impacts compared with radioligand assays. Additionally, FP assays are easily miniaturized, do not require laborious filtration steps, and can be executed in a homogeneous (mix-and-read) fashion, thus leading to assays that are truly high-throughput. While there are clear incentives to move from radioligand assays to FP assays, a major challenge is the need to develop a fluorescent ligand that has high affinity for the receptor of interest. Usually this is accomplished through synthetic modification of a high affinity ligand so that it can accommodate covalent coupling to a fluorescent dye without negatively perturbing the binding affinity of the parent ligand (for recent examples, see refs 14−17). This is an empirical process, but the likelihood of success is increased by use of existing SAR, binding models, and crystallographic data when available. Herein, we describe the development of a family of fluorescent ligands that bind the hERG channel with high affinity and, when bound, give a robust FP signal.

Ligand Design, Synthesis, and SAR

The antiarrhythmic agent dofetilide[18] (**1**) was chosen as the scaffold for fluorescent analogue development. Dofetilide is a member of the methanesulfonanilide (MSA) class of antiarrhythmic drugs and is marketed under the brand name Tikoyan. It binds to the hERG channel with high affinity[19] and potently blocks channel current in a patch clamp assay.[4,19] *N*-Desmethyldofetilide[20] (**2**) was alkylated with 4-chloro-7-nitrobenzoxadiazole (NBD chloride) to produce fluorescent product **3** (Scheme 1). When tested in a standard scintillation proximity assay (SPA) that uses ^{3}H dofetilide as a radioligand, **3** exhibited a 15-fold increase in affinity for hERG channel relative to **1** (Table 1). While **3** served as an excellent proof-of-concept compound, it did not show a useful FP signal upon binding. Hence, two other dyes commonly used in FP assays were examined. Activation of 5- and 6-carboxyfluorescein and 5-carboxytetramethylrhodamine (TMR) with HATU (*N*-[(dimethylamino)-1*H*-1,2,3-triazolo[4,5-*b*]pyridin-1-ylmethylene]-hexafluorophosphate *N*-oxide) followed by reaction with **2** produced fluorescent derivatives **4** and **5**, respectively. These analogues showed poor affinity for the hERG channel in the

Scheme 1. Synthesis of Fluorescent Analogues of Dofetilide by Direct Acylation or Arylation of the Central Core Nitrogen[a]

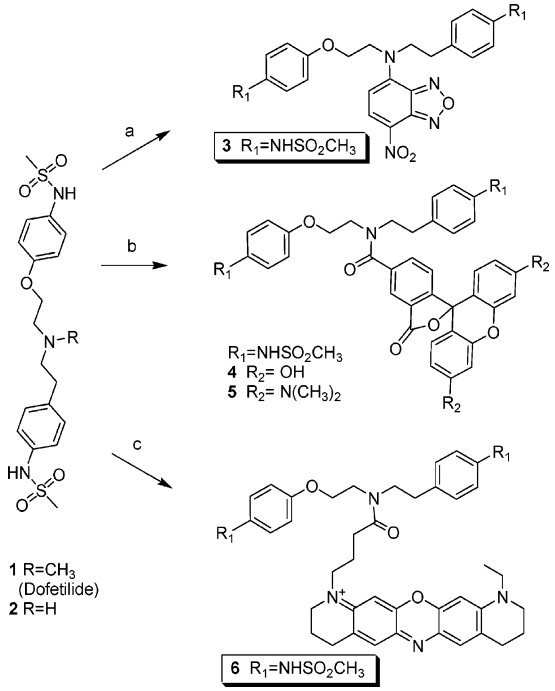

[a]Reagents and conditions: (a) NBD chloride (1.0 equiv), DMF, 2 h, 41%; (b) 5- and 6-carboxyfluorescein (mixed isomers) or 5-carboxy TMR (1.0 equiv), HATU (1.0 equiv), HOAt (1.0 equiv), 10% DIEA in DMF, 4 h, 5−40%; (c) MR121 (0.6 equiv), HATU (1.0 equiv), HOAt (1.0 equiv), DIEA in DMF, 4 h, 35%.

Table 1. SPA Derived hERG Channel Affinities of Fluorescent Dofetilide Analogues[a]

compd	K_i (nM)[b]	standard deviation (nM)	*n*
1	6.4	2.7	280
3	0.39	0.08	4
4	980		1[c]
5	>1000		2
6	3.6	0.4	2
10a	7300		2
10b	160	70	2
10c	18	2.0	2
10d	13	2.0	2
10e	7.0	0.8	4
12a	19	4.4	2
12b	10	4.3	3
13	15	15	4
14	89	51	4
15	>1000		1

[a] K_i values determined from competition binding experiments in an SPA format using HEK293 cell membranes expressing hERG protein and [^{3}H]dofetilide tracer.[40] [b] Reported K_i values are the arithmetic mean of multiple experiments performed in triplicate. [c] A second experiment showed a similar degree of inhibition but did not allow for a calculated K_i.

Scheme 2. Synthesis of Fluorescent Dofetilide Analogues with Variable-Length Spacers[a]

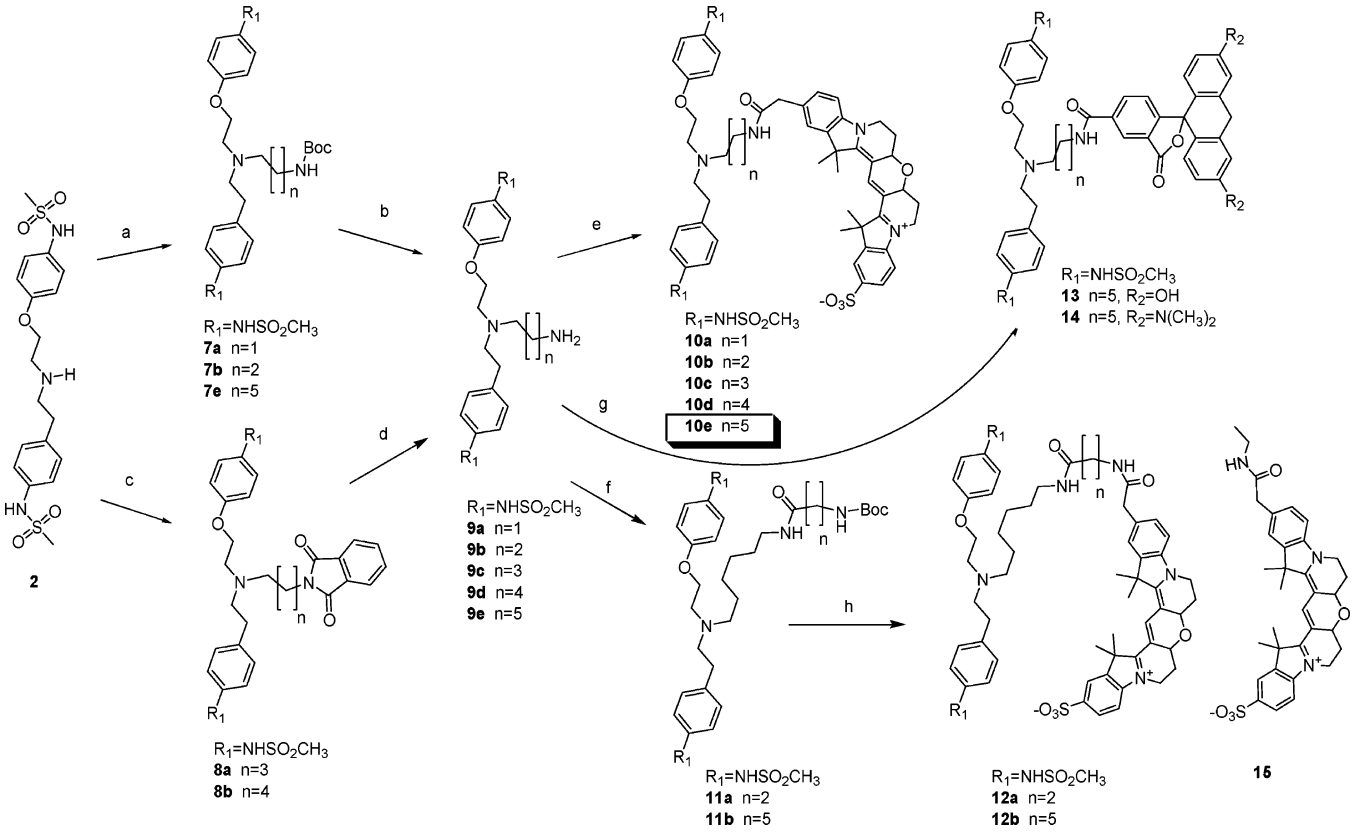

[a] Reagents and conditions: (a) Boc amino aldehyde (2.0 equiv), $NaBH(OAc)_3$ (2.0 equiv), 4:1 DCE/THF, room temp, 16 h, 47%; (b) TFA, room temp, 5 min, >95%; (c) bromoalkylphthalimide (2.4 equiv), Na_2CO_3, ACN, reflux, 4 h, 53%; (d) hydrazine (6 equiv), methanol, reflux, 2 h, 58%; (e) Cy3B NHS ester (1.0 equiv), 5% DIEA in DMF, room temp, 15 min, 86%; (f) Boc amino acid (0.75 equiv), HBTU (0.75 equiv), 10% DIEA in NMP, room temp, 30 min, 57%; (g) fluorescein NHS ester or TMR NHS ester (1.0 equiv), 5% DIEA in DMF, room temp, 15 min; (h) (i) TFA, 5 min, (ii) Cy3B NHS ester (1.1 equiv), 20% DIEA in DMF, room temp, 1 h, 29%.

SPA. Next, derivatives that feature spacer groups between the dye and the central nitrogen of **2** were synthesized. The red-shifted dye MR121 (1-(3-carboxypropyl)-11-ethyl-1,2,3,4,8,9,-10,11-octahydrodipyrido[3,2-*b*:2′,3′-*i*]phenoxazin-13-ium inner salt) includes a butyric acid spacer, which following activation with HATU acylates the secondary nitrogen of **2**. The resulting compound **6** has an hERG channel affinity close to that of dofetilide.

Many of the commercially available dyes useful for FP assays are sold as *N*-hydroxysuccinimide (NHS) esters. In order to make conjugates with these dyes, hydrocarbon spacers with protected terminal amines were prepared. As shown in Scheme 2, **2** undergoes reductive alkylation with C_2, C_3, and C_6 *tert*-butyloxycarbonyl (Boc) protected amino aldehydes to give Boc protected amines **7a**, **7b**, and **7e** in good yield. Removal of the Boc groups of **7a**,**b**,**e** with trifluoroacetic acid (TFA) provided compounds **9a**,**b**,**e** as their TFA salts. The C_4 and C_5 Boc protected amino aldehydes reacted poorly with **2**, presumably because of their tendency to form cyclic hemiaminals. The C_4 and C_5 protected amines were obtained via alkylation of **2** with phthalimide protected aminoalkyl bromides to give phthalimides **8a**,**b**. Deprotection with hydrazine provided amines **9c**,**d** as free bases. The synthesis of conjugates of **2** with longer amide-containing linkers was accomplished by reaction of **9e** with either *N*-Boc-3-aminopropionic acid or *N*-Boc-6-aminocaproic acid using HBTU (2-(1*H*-benzotriazol-1-yl)-1,1,3,3-tetramethyluronium hexafluorophosphate) activation to give Boc protected conjugates **11a**,**b**, respectively.

Cy3B (2-(carboxymethyl)-6,7,9,10,16,18-hexahydro-16,16,-18,18-tetramethyl-14-sulfopyrano[3″,2″:3,4;5″,6″:3′,4′]dipyrido-[1,2-*a*:1′,2′-*a*′]diindol-5-ium, inner salt) conjugates **10a**−**e** were prepared by mixing amines **9a**−**e** each with an equivalent of Cy3B NHS ester in DMF/DIEA, followed by purification with reverse-phase HPLC. The *N*-ethylamide of Cy3B (**15**) was prepared as a control compound in the same manner. Conjugates **12a**,**b** were prepared similarly by first deblocking **11a**,**b** with TFA and reaction with Cy3B NHS ester. Fluorescein and TMR conjugates **13** and **14** were prepared by reaction of **9e** with fluorescein and TMR NHS esters, respectively.

Compound purity of fluorescent derivatives of **2** was assayed by two analytical HPLC methods as described in Supporting Information. All compounds exceeded 95% purity except **4** (88% as a 4:3 mixture of regioisomers) and **10a** (82%). Yields were calculated on the basis of UV absorbance at λ_{max} in neutral aqueous buffers. Samples were then aliquoted, lyophilized as TFA salts, and redissolved in water for testing.

Table 1 displays the SPA measured binding affinities of all fluorescent derivatives of **2**, and several trends are worthy of note. First, for conjugates **3**−**5**, there is a marked affinity dependence on the structure of the attached dye. NBD derivative **3** experiences a 15-fold increase in affinity over dofetilide, while fluorescein and TMR derivatives **4** and **5** suffer more than a 150-fold decrease in affinity. Second, for Cy3B conjugates **10a**−**e** and **12a**,**b**, a consistent affinity dependence on spacer length was observed. Moving from a two-methylene spacer for compound **10a** to a four-methylene spacer for compound **10c** resulted in a 400-fold increase in affinity. Increasing the spacer length from four to six methylenes gave a modest 3-fold increase in affinity to the maximum observed for conjugate **10e**, which is equipotent to dofetilide. Additional linker length via amide-

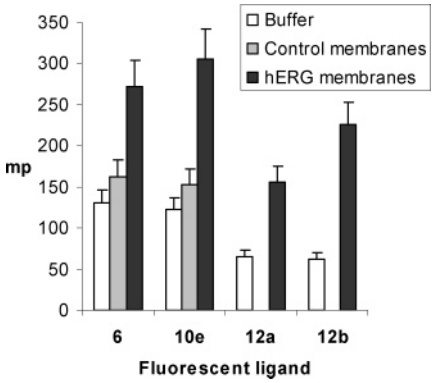

Figure 1. Change in FP upon ligand binding to hERG channel. Shown are FP signals for Cy3B ligands **10e** (3.0 nM), **12a** (2.0 nM), and **12b** (2.0 nM) and MR121 ligand **6** (5.0 nM) absent membranes (white bars), with hERG transfected HEK293 membranes (black bars) or with control HEK293 membranes transfected with irrelevant control (serotonin transporter, gray bars). Error bars represent standard deviations from experiments run in triplicate.

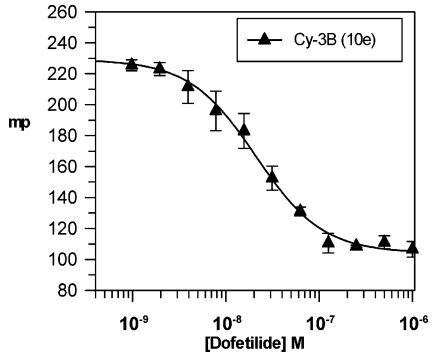

Figure 2. FP competition binding experiment. The FP response for Cy3B ligand **10e** as a function of [**1**] is shown. Calculated K_i for **1** is 8.0 nM, and the Hill slope is 1.2. Error bars represent standard deviations for experiments run in triplicate.

containing spacers (**12a**,**b**) did not result in further increases in affinity. As expected, no binding was detected for negative control Cy3B compound **15**. Third, even with optimal spacer length, there appears to be an affinity dependence on conjugate dye. Exchanging the Cy3B dye of **10e** for fluorescein (**13**) did not significantly alter binding, but the structurally similar dye TMR (**14**) caused a 12-fold affinity reduction.

Fluorescence Polarization

Because of their high affinity for hERG channel and their desirable spectral properties, ligands **6**, **10e**, **12a**, and **12b** were selected for further evaluation. NBD ligand **3** displayed low fluorescence intensity when bound to receptor and was not pursued further. In order to detect a robust change in polarization upon receptor binding, a HEK293 cell line that highly expresses hERG protein was developed.[21] Figure 1 shows the change in FP signal upon Cy3B ligands **10e**, **12a**, **12b**, and MR121 ligand **6** binding to hERG channel membranes. Membranes lacking the hERG protein were used as a specificity control. For all four ligands a robust fluorescence polarization effect was observed. Ligands **10e** and **12b** showed more than a 100% increase in polarization over background, while the effect with ligands **6** and **12a** was slightly less pronounced. Interestingly, **12b** did not suffer a loss in polarization despite its long and flexible 14-atom linker.

Because of its lower background signal and better assay performance, **10e** was chosen for full pharmacological characterization. In competition experiments with increasing concentrations of dofetilide, **10e** shows the expected sigmoidal FP response curve with a Hill coefficient of 1.2 (Figure 2). The calculated dofetilide K_i [22] from the experiment is 8.0 nM. The arithmetic mean K_i for multiple experiments is 7.7 nM (n = 610, average Hill slope of 1.04), essentially equivalent to the SPA derived K_i value of 6.4 nM. In order to judge the performance of **10e** as a tracer FP ligand, it was tested against other known hERG channel binding molecules with affinities in the low nanomolar to low micromolar range. Table 2 shows the FP and SPA derived K_i values for astemizole, E-4031, bepridil, mibefradil, and clozapine and compares them to values reported in the literature. Four of these hERG channel inhibitors showed excellent agreement between the two assay formats. The lone exception was high-affinity inhibitor astemizole, which registered a 4.4-fold higher K_i in the SPA format. The FP derived K_i values are also in agreement with those reported by Diaz et al.,[19] and the rank order of compound affinities is the same in all three assays.

Table 2. SPA and FP-Derived K_i Values for Literature Standard hERG Channel Inhibitors[a]

compd	FP K_i (nM)[b]	SPA K_i (nM)[c]	SPA/FP	literature (nM)[d]
astemizole	2.9(0.9)	12.8(3.0)	4.4	2
dofetilide	7.7(4.4)[e]	6.4(2.7)[f]	0.91	10
E-4031	18.7(3.8)	19.4(3.1)	1.04	30
bepridil	184(25)	291(63)	1.6	170−450
mibefradil	190(32)	353(97)	1.85	660−890
clozapine	4060(840)	3080(900)	0.77	1200−5800

[a] Comparison of K_i values determined from competition binding experiments in an SPA or FP format. Reported K_i values are the arithmetic mean of multiple experiments performed in triplicate. Standard deviations are in parentheses. [b] FP assay using **10e** as fluorescent tracer. [c] SPA as in Table 1. [d] From Diaz et al.[19] Single K_i values from measurements at 10 mM K^+. Range reflects K_i values measured at 60 and 5 mM K^+. [e] The K_i values reported for dofetilide are the arithmetic mean of experiments run regularly over many months (n = 610). [f] From Table 1.

Table 3. Patch Clamp IC_{50} and τ Values and Apparent Permeability Data[a]

compd	patch clamp IC_{50} (nM)[b]	SPA K_i (nM)[c]	τ for onset of block (s)[d]	P_{app} [e] absorptive ($\times 10^{-6}$ cm/s)	P_{app} [e] secretory ($\times 10^{-6}$ cm/s)[e]
1	9.2	6.4	182(30)	15.7(2.6)	14.3(2.3)
3	<3	0.39	575*(42)	3.7(0.9)	18.0(2.6)
10e	310	7.0	316*(35)	5.4(0.2)	4.8(0.9)

[a] Comparison of patch clamp IC_{50} and τ values to apparent cell permeability as determined in a Caco-2 assay. [b] IC_{50} values determined from data shown in Figure 3D. [c] SPA data from Table 1. [d] Time constants (and standard error values) derived from time course of onset of current block at concentrations that produced 80% inhibition of the hERG channel current (25 nM **1**, 3.0 nM **3,** and 1000 nM **10e**). Asterisks denote a significant difference from **1** (see Experimental Section for description of analysis). [e] Caco-2 permeability data determined in the absorptive and secretory transport directions in the presence of 5 μM cyclosporin A. Values represent the mean (and standard deviations in parentheses) of two separate experiments in triplicate.

Patch Clamp Electrophysiology and Cell Permeability

To confirm that the hERG channel binding activities of ligands **3** and **10e** translate to actual functional blockade of potassium current, ligands were tested using patch clamp electrophysiology.[23] Both **3** and **10e** blocked hERG channel current but at different potencies and with slower kinetics when compared to **1** (Figure 3A−C, Table 3). By observation of the percent inhibition at apparent steady-state block as a function of ligand concentration, IC_{50} values of 9.2, <3, and 310 nM were determined for ligands **1**, **3**, and **10e**, respectively (Figure 3D). The IC_{50} value determined for **1** was comparable to the

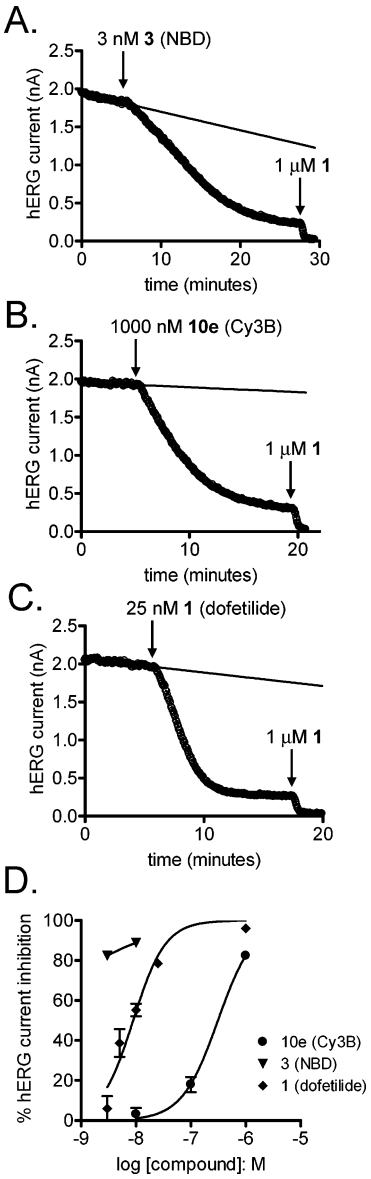

Figure 3. Functional blockade of hERG channel currents assessed by whole-cell patch clamp. The peak of the current tail is plotted as a function of time, and typical examples of current blockade by 3 nM **3** (A), 1000 nM **10e** (B), and 25 nM **1** (C) are shown at concentrations that induced approximately 80% hERG channel current inhibition. Initiation of continuous ligand perfusion is indicated by an arrow, and extrapolation of the rundown of the control current is depicted with a solid line. Upon achieving an apparent steady state of ligand blockade, cells were perfused with 1 μM dofetilide to demonstrate complete inhibition of current. (D) Percent inhibition of the hERG channel current at apparent steady state is plotted as a function of ligand concentration. Results for **1** and **10e** were fit with the Hill equation (solid line) to estimate IC_{50} values. Data are mean $\pm$ SEM; $n \geq 4$ except for 10 nM **10e** for which $n = 2$ cells.

SPA K_i of 6.4 nM, while the IC_{50} of **10e** was 40-fold less potent than the SPA K_i of 7.0 nM. An exact IC_{50} value for **3** could not be determined because of slow kinetics of onset of block at concentrations below 3 nM ($\tau = 575 \pm 42$ s at 3.0 nM).

Since hERG channel ligands are believed to block the channel from the cytoplasmic face of the pore,[4,24] we asked if slow blocking kinetics of **3** and **10e** and reduced potency of **10e** could be attributed to poor membrane permeability conferred by the fluorescence tags. All three ligands were tested in a standard Caco-2 permeability assay[25] in which 5 μM cyclosporin A was added as a nonspecific inhibitor of cell transporters.[26] Consistent with this hypothesis, **10e** displayed low permeability in both absorptive and secretory transport directions while **1** was moderately permeable (Table 3). NBD compound **3** showed asymmetric permeability, low in the absorptive direction and moderate in the secretory direction. The results suggest that **10e** and **3** may have reduced access to the intracellular compartment of the HEK293 cells used in patch clamp experiments.

Molecular Modeling

A homology model of hERG channel was created using Modeler 6,[27] with the crystal structure of the bacterial potassium channel KcsA[28] as the template structure. Twenty homology models were generated. On the basis of energy, visual inspection, and analysis using Procheck,[29] the best model was selected. The conformations of critical ligand binding residues[30] Tyr652 and Phe656 were adjusted to the most commonly found conformations in the PDB using Quanta2000. Compounds **3** and **10e** were separately docked in the homology model cavity without restraints using GOLD.[31] The ligand dockings were scored using the GoldScore function, with the top 20 binding modes retained. Figure 4A shows the 20 energetically most favorable docked conformations of compound **3**. In 17 of these models, one of the two nonequivalent methanesulfonanilide (MSA) groups of **3** rests between juxtaposed residues Phe656 from each of the four protein subunits. Figure 4B shows the three docked conformations of **3** with the highest GoldScore values. While there are significant differences between these models, all feature a MSA low in the channel pore. Interestingly three of the top 20 models predict an alternative conformation with the NBD group interacting with Phe656 and both MSA groups closer to Tyr652 (not shown). In Figure 4C the docked conformation of **10e** with the highest GoldScore is shown along with a model of **3** with the second highest GoldScore. The polycyclic Cy3B dye of **10e** is predicted to occupy the water-filled cavity[28] within the pore. Other conformations where the Cy3B dye of **10e** rests in the channel pore and interacts with Phe656 were also observed (not shown).

Discussion

FP assays are finding increasing utility in drug discovery in part because of their compatibility with miniaturized formats for HTS. A general limitation when converting small-molecule radioligand assays to FP assays is the need to develop high-affinity small-molecule fluorescent conjugates. The major challenge is to append covalently a fluorescent dye to a known ligand without suffering a significant loss of binding affinity. In contrast to radioligand binding experiments, FP requires that most of the added tracer ligand be bound to give robust polarization signal. To achieve this endpoint with a fluorescent ligand of moderate affinity (0.1−1 μM), significant increases in receptor concentration may be necessary, perhaps to the point where HTS becomes impractical. In addition to preserving affinity, it is preferable that the reporter ligand retain the pharmacological function of the parent ligand as well.

Ligand development is empirical and iterative[16] in nature, but success rates can be enhanced by effective use of preexisting small-molecule SAR, detailed ligand−receptor models, and ligand−receptor cocrystal structures. For the development of FP ligands from **1**, we considered the three nonequivalent methyl groups as synthetic handles for dye linkage. Unpublished results from these labs show that even modest modifications to either of the MSA methyl groups result in >10-fold loss in hERG channel affinity, so synthetic efforts were focused on replace-

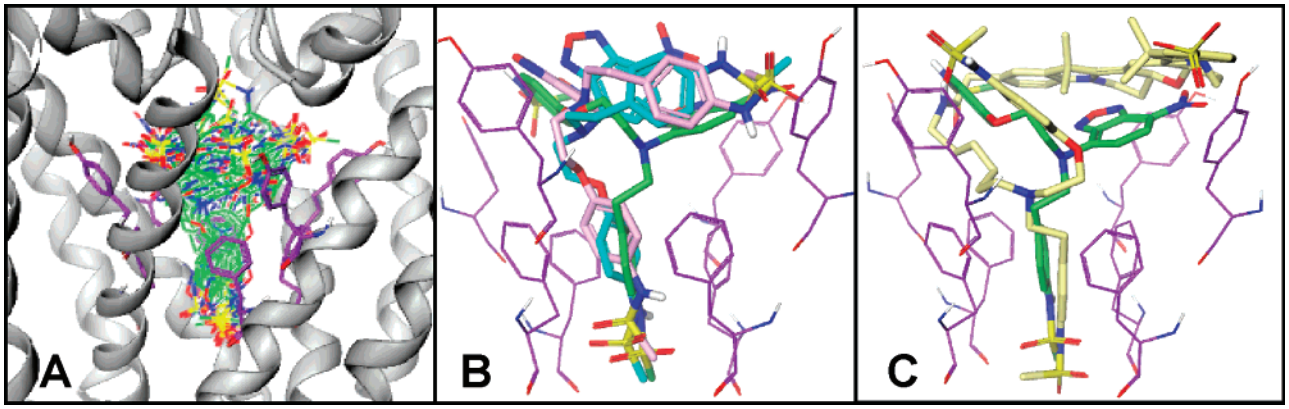

Figure 4. Homology model of hERG protein with models of **3** and **10e** docked into the pore. (A) Tetrameric hERG protein homology model with channel-forming helices and loops rendered in gray ribbon style and inner pore aromatic residues Tyr652 and Phe656 shown in dark purple. The intracellular opening of the channel is at the bottom of the figure. The 20 docked conformations of **3** with the highest GoldScore values are displayed in the channel pore. The MSA sulfur atoms in yellow show good overlap below the Phe656 residues. (B) Close-up view of the three docked conformations of **3** with the highest GoldScore values in light-purple, green, and blue. Pore residues Tyr652 and Phe656 are shown in dark-purple. (C) Close-up view of **10e** in gold and **3** in green. Model predicts a high degree of overlap of the lower MSA groups. The Cy3B group is shown edge-on (orthogonal to the plane of the figure) in the pore cavity above residue Tyr652.

ments of the methyl group at the central tertiary amine of **1**. This led to ligands with poor affinity (**4**, **5**, **10a**), moderate affinity (**10b**, **14**), high affinity (**6**, **10c**−**e**, **12a**, **12b**, **13**), and very high affinity (**3**). Among the high-affinity conjugates described, Cy3B conjugate **10e** was judged to be superior by virtue of its excellent spectral properties and its performance in FP competition binding experiments. MR121 conjugate **6** performed well in FP assay development experiments, but **10e** had a higher statistical *Z*-factor[32] value and is preferred (unpublished results).

Known hERG channel blockers dofetilide, E-4031, bepridil, mibefradil, and clozapine were shown to compete equally well with [^{3}H]dofetilide or **10e** in SPA or FP formats, respectively (Table 2). The compounds tested feature hERG channel affinities from low nanomolar to low micromolar concentrations, demonstrating consistent results over a dynamic range of at least 3 orders of magnitude. Reassuringly, the values reported here correspond well with those from another laboratory.[19] The high-affinity blocker astemizole was the only compound to show greater than a 2-fold difference between the two formats. The K_i for astemizole binding to hERG channel membranes is reported to vary more than 10-fold with changes in potassium ion concentration, but this probably does not explain the discrepancy reported here because all experiments were run at 10 mM K^+. Nonetheless, the rank order of all six compounds is the same between the two assays. A comprehensive assay validation study using a panel of well-known hERG channel binding compounds has been conducted and is reported in a separate manuscript.[21] The data highlight that the K_i values determined for a range of known hERG channel blockers (ranging from low nanomolar to tens of micromolar concentration) are equivalent to those obtained with radiometric methods.

To be predictive of functional hERG channel blockade, an ideal FP ligand should not only have a high affinity for the hERG protein but also bind in a manner that inhibits the channel current. In patch clamp electrophysiology experiments, **10e** reversibly inhibited hERG channel currents[21] in a use-dependent manner similar to **1**. However, **3** and **10e** displayed slower onset of channel block (Figure 3A−C, Table 3). At concentrations that induced 80% current inhibition, time constants (τ) for onset of block were significantly larger for **3** and **10e** than for **1**. Dofetilide and similar molecules are believed to block current by crossing the cell membrane and entering the channel via the cytoplasmic face of the protein.[4,5,24] Because **3** and **10e** displayed low permeability in a Caco-2 assay compared to the moderately permeable dofetilide, the discrepancy in kinetics of block may be due in part to the different rates of intracellular accumulation of the compounds. However, the permeability data cannot fully account for the observed differences in patch clamp IC_{50} values. Ligand **3** is 18-fold more potent than **10e** in the SPA and at least 100-fold more potent in patch clamp, but **3** and **10e** show similar cellular permeability across Caco-2 cells in the presence of cyclosporin A. Since FP ligand binding studies are performed using homogenized cell membrane vesicles of variable orientation (normal and inside out), membrane permeation is not required for **10e** to access the ligand binding site. Therefore, reduced membrane permeation should have little impact on the effectiveness of **10e** as an FP ligand. One would expect that FP derived binding data would be as predictive of functional hERG channel block as a radioligand derived binding data, and this is indeed the case. The FP derived K_i values for 18 known hERG channel binding compounds were measured and compared to their patch clamp derived IC_{50} values.[21] Strong correlation was observed for compounds with potencies ranging from 8 nM to >10 μM.

It is important to note some key differences in **10e** vs ligand **3** permeability observed from the Caco-2 studies. For **10e**, Caco-2 permeability is low because passive permeability was found to be low. From these studies, one would predict that cellular permeability of **10e** would be low in other cell types. Conversely, ligand **3** Caco-2 permeability is low in some or all cell types because of attenuation via efflux transport rather than solely because of poor passive membrane permeability. It is likely that the absorptive cellular permeability determined for **3** underestimates the true passive membrane permeability of this compound because of the attenuating activity of efflux transporters not inhibited by cyclosporin A (it is, however, impossible to determine from these experimental results if the observed asymmetry was due to attenuation and/or enhancement of **3** passive membrane permeability during absorptive vs secretory transport). Therefore, from the Caco-2 studies, the cellular permeability of **3** would be expected to depend on both passive permeability and expression of efflux transporters in the cell type. There are differences in transporter expression between Caco-2 and HEK cells (unpublished results), and it is possible that the efflux transporter responsible for imparting the observed asymmetry to ligand **3** in Caco-2 cells may not be active, or could show less activity vs Caco-2 than in HEK cells.

Conversely, if the passive membrane permeability of ligands **3** and **10e** is comparable, it is possible that the HEK cells used in patch clamp are able to selectively efflux **10e** but not ligand **3**. Each scenario would give rise to differences in permeability between the compounds and subsequent differences in intracellular accumulation over time and observed potency between compounds **10e** and **3**.

To rationalize our SAR, we referred to models of methanesulfonanilide (MSA) compounds docked into the channel of a hERG protein homology model, which was built upon the crystal structure of the bacterial potassium channel KcsA.[33,34] The KcsA and subsequent potassium channel crystal structures demonstrate that pores have conserved features, including an intracellular membrane proximal inner pore about 18 Å in length, a central water filled cavity about 10 Å in diameter, and an extracellular membrane proximal selectivity filter.[28] Interpretation of the SAR reported here is greatly simplified by assuming that the binding modes of fluorescent dofetilide derivatives are not substantially perturbed from the consensus MSA binding mode. Our models and others[35,36] predict that MSA inhibitors bind in extended conformations with one of the MSA groups sandwiched between critical binding Phe656 residues[30] from each protein subunit. Computational experiments in which high-affinity analogues **3** and **10e** were docked into a hERG channel homology model were performed, and low-energy bound conformations are shown in Figure 4. The MSA-Phe656 interactions appear to anchor the dofetilide core within the inner pore (Figure 4A). Low-energy docked conformations of **3** (Figure 4B) lack overtly unfavorable nonbonded interactions with the channel but do not reveal any obvious favorable interactions that would explain the 15-fold increase in affinity relative to **1.** Most likely the jump in affinity is due at least in part to the significant increase in hydrophobicity that the NBD confers upon **3** relative to **1**. Once bound, the NBD group is available to interact with Tyr652 or other hydrophobic residues. Docked conformations of **3** where the NBD group interacts with Phe656 and both MSA groups interact with Tyr652 were also observed (data not shown). These do not match well to consensus MSA binding models but should not be dismissed entirely.

For high-affinity conjugates **6**, **10c**−**e**, and **12a**,**b** (SPA K_i < 25nM) to bind in a mode that is consistent with models proposed for MSA inhibitors, the polycyclic conjugate dyes need to occupy space outside the inner pore. An obvious compartment is the cavity just above the inner pore. hERG protein homology models predict that hydrophobic residues line the cavity, creating a suitable environment for aromatic dyes.[28] The docked model of **10e** shown in Figure 4C orients the Cy3B moiety in the central cavity of the pore with the planar fused ring system orthogonal to the pore axis. This model requires a flexible spacer between the dye and dofetilide core and therefore is consistent with the spacer length dependence observed for analogues **10a**−**e**. Alternative conformations where the dye resides in the lower channel or outside the pore cannot be ruled out. Testing for the molecular determinants of blockade using mutagenesis of the channel would lead to greater certainty that the binding does occur at similar residues as does dofetilide.

The KcsA structure and hence the homology model shown here exist in closed conformation. Other workers have proposed hERG channel homology models based on open potassium channel structures.[37,38] Those models have larger pore openings that allow docked compounds to reside lower in the pore (closer to the cytoplasmic opening), but the predicted interactions with binding residue Phe656 are qualitatively similar. Open channel homology models might also accommodate a ligand binding model where a long flexible spacer threads down through the inner pore and conjugate dye rests in the cytoplasm. However, with this orientation one would predict that channel affinity would be relatively independent of conjugate dye. The decrease in affinity observed when the Cy3B of **10e** is exchanged for TMR in **14** indicates that the dyes are interacting with hERG protein residues. The cavity-filled model in Figure 4C seems more consistent with this result. Also, analogue **12b** has a flexible 14-atom spacer between the dofetilide core and the Cy3B dye and yet retains the magnitude of polarization observed with **10e** when bound (Figure 1). A model with the dye in the cytoplasm would allow for free dye rotation and perhaps a loss of polarization. A cavity-packed model would not allow for free rotation, and polarization would be preserved.

In summary, novel fluorescent analogues of dofetilide (**1**) have been discovered. Several analogues have affinity for hERG channel that equals or exceeds that measured for **1**. Most notably, the Cy3B ligand **10e** and the MR121 ligand **6** show robust increases in polarization when bound to membranes prepared from HEK293 cells that overexpress hERG protein. The excellent spectral properties of these ligands have enabled the development of an economical HT FP binding assay that is predictive of test compounds' ability to block hERG channel current.[21] We anticipate that this or similar assays will become standard medicinal chemistry methods for early assessment of potential QT prolongation liabilities.

Experimental Section

Chemistry. Reactions were performed using commercially available reagents from Aldrich (Milwaukee, WI) and solvents from JT Baker or Applied Biosystems Inc. (Foster City, CA) that were used as purchased. 5-Carboxyfluorescein NHS ester, 5-carboxy TMR NHS ester, 5- and 6-carboxyfluorescein (mixed isomers), 5-carboxy TMR, and NBD chloride were from Molecular Probes (Eugene, OR). Cy3B NHS ester was from GE Healthcare (Amersham Biosciences Piscataway, NJ). MR121 was purchased from Roche Biosciences (NJ). A synthesis of *N*-desmethyldofetilide[20] (**2**) has been reported. Boc amino aldehydes were prepared from commercially available Boc amino alcohols as described.[39] HATU and aminomethylpolystyrene resin were purchased from EMD Biosciences (San Diego, CA). Astemizole, bepridil hydrochloride, clozapine, mibefradil dihydrochloride hydrate, and E-4031 (*N*-[4-[[1-[2-(6-methyl-2-pyridinyl)ethyl]-4-piperidinyl]carbonyl]phenyl] methanesulfonamide dihydrochloride) are sold by Sigma (St. Louis, MO). Silica gel chromatography was performed on a Biotage flash column gradient pump system using 15 cm long columns. NMR was performed on a 400 MHz field strength spectrometer from Varian Inc. (Palo Alto, CA) in CD_3OD. Chemical shifts are reported in parts per million (ppm). Methanol solvent peaks were used as references (^1H = 3.32 ppm, ^{13}C = 49.0 ppm). High-resolution mass spectrometry was peformed in electrospray mode. Analytical samples for liquid chromatography electrospray mass spectrometry (LC ESMS) were dissolved at 4 μM in 1:1 ACN/H_2O. An amount of 5 μL each was injected onto an Aquity 2.1 mm × 100 mm UPLC 1.7 Å BEH C18 column and eluted using a linear gradient from 100% 0.1% formic acid/water to 100% ACN over 10 min with a flow rate of 0.4 mL/min. Mass detection was performed using a Micromass LCT spectrometer employing external calibration with sodium iodide/cesium iodide clusters to determine experimental masses. Observed peaks were evaluated by summing those scans at one-half peak height. HRMS experiments were performed using electrospray ionization on a Micromass MUX-LCTP instrument that had been calibrated with leucine enkaphalin as the lock mass reference. Compound purity was assessed by complementary HPLC methods: C18 reverse-phase chromatography and hydrophilic interaction chromatography using diode array UV detection as described in Supporting Information. All compounds met or exceeded 95% purity except **4** (roughly a 4:3 mixture

of 5- and 6-carboxyfluorescein isomers) and **10a** (82% pure). Preparative HPLC purifications were performed with either a Vydac (Hesperia, CA) C18 column (part number 218TP1022) or a Vydac semipreparative diphenyl column (Vydac part number 219TP510) using a 0.1% TFA/water and neat ACN elution gradient. Yields for fluorescent products were calculated from UV absorbance measurements performed on HPLC purified products. Briefly, an aliquot of pooled product in HPLC eluent was diluted into pH 7 aqueous buffer and the absorbance measured at the following wavelengths: 466 nm for compound **3** (ϵ = 22 000 L mol^{-1} cm^{-1}); 492 nm for **4** and **13** (ϵ = 75 000 L mol^{-1} cm^{-1}); 550 nm for **5** and **14** (ϵ = 80 000 L mol^{-1} cm^{-1}); 660 nm for **6** (ϵ = 100 000 L mol^{-1} cm^{-1}); 562 nm for **10a**−**e** and **12a**,**b** (ϵ = 130 000 L mol^{-1} cm^{-1}).

***N*-(4-{2-[[2-(4-Methanesulfonylaminophenoxy)ethyl](7-nitrobenzo[1,2,5]oxadiazol-4-yl)amino]ethyl}phenyl)-methanesulfonamide (3).** To a solution of 25.5 mg (60 μmol) of *N*-desmethyldofetilide (**2**)[20] in 0.3 mL of DMF was added 12 mg (60 μmol) of 4-chloro-7-nitrobenz-2-oxa-1,3-diazole (NBD chloride). After 2 h the reaction was judged by LCMS to be >90% consumed. The reaction mixture was directly purified by preparative C18 HPLC. Collected fractions were analyzed by analytical LCMS, and those judged as having adequate purity were pooled. Product yield was calculated as 14.5 mg (41%), and the pooled fractions were lyophilized to dryness. ^{1}H NMR (CD_3OD): δ 8.49 (d, 1H, J = 10 Hz), 7.26 (d, 2H, J = 8.3 Hz), 7.15 (d, 2H, J = 8.3 Hz), 7.14 (d, 2H, J = 8.8 Hz), 6.87 (d, 2H, J = 8.8 Hz), 6.53 (d, 1H, J = 10 Hz), 4.16 (m 4H), 3.26 (m, 2H), 3.05 (t, 2H, J = 7.0 Hz), 2.87 (s, 3H), 2.82 (s, 3H). ESMS: calculated *m*/*z* for $(MH)^+$ = 591.13, found = 591.10. HRMS: *m*/*z* calculated for $C_{24}H_{27}N_6O_8S_2$ $(MH)^+$ = 591.1326, found = 591.1288.

Synthesis of 5 (5-Carboxy TMR Conjugate of 2), TFA Salt. To a solution of 4.3 mg (10 μmol) of 5-carboxy TMR and 0.10 mL of DMF were added 3.8 mg (10 μmol) of HATU and 20 μL of a 0.5 M solution of HOAt (10 μmol) in DMF. Then 20 μL (120 μmol) DIEA was added, and after 1 min the resulting deep-red solution was added to a solution of 4.3 mg (12 μmol) of **2** dissolved in 0.20 mL of DMF. After 20 min, the product was purified by direct injection of the reaction mixture onto a semipreparative diphenyl column. Collected fractions were analyzed by HPLC, and appropriate fractions were pooled and lyophilized. Calculated product yield = 3.32 mg (40%). ESMS: calculated *m*/*z* for $(MH)^+$ = 840.27, found = 840.11. HRMS: *m*/*z* calculated for $C_{43}H_{46}N_5O_9S_2$ $(MH)^+$ = 840.2726, found = 840.2761.

Synthesis of 4 (5- and 6-Carboxyfluorescein Conjugates of 2). The procedure is similar to the procedure for **5**. Calculated product yield = 5%. ESMS: calculated *m*/*z* for $(MH)^+$ = 786.18, found = 786.12. HRMS: *m*/*z* calculated for $C_{39}H_{36}N_3O_{11}S_2$ $(MH)^+$ = 786.1782, found = 786.1851

Synthesis of 6 (MR121 Conjugate of 2), TFA Salt. The procedure is similar to the procedure for **5**. Calculated product yield = 35%. ESMS: calculated *m*/*z* for $(M)^+$ = 815.33, found = 815.24. HRMS: *m*/*z* calculated for $C_{42}H_{51}N_6O_7S_2$ $(M)^+$ = 815.3249, found = 815.3273.

***tert*-Butyl 3-((4-(Methylsulfonamido)phenethyl)(2-(4-(methylsulfonamido)phenoxy)ethyl)amino)propylcarbamate (7b).** 3-[(*tert*-Butoxycarbonyl)-amino]propanal[39] (81 mg, 468 μmol) in 8 mL of 1,2-dichloroethane was mixed with 100 mg (234 μmol) of **2** followed by 100 mg (468 μmol) of sodium triacetoxyborohydride. To enhance solubility, 2 mL of tetrahydrofuran was added to the mixture which was stirred at room temperature. After 40 min, 50 mg (234 μmol) of sodium triacetoxyborohydride was added. After a total of 5 h, 100 mg (468 μmol) of sodium triacetoxyborohydride was added. After 16 h, excess residual aldehyde was absorbed by the addition of 100 mg of aminomethylpolystyrene resin followed by stirring for 30 min. The resin was removed by filtration, and the remaining filtrate was diluted with 50 mL of water and extracted with 100 mL of dichloromethane. The organic layer was washed with 1 × 50 mL saturated NaCl, dried over $MgSO_4$, filtered, and concentrated to an oily solid. Purification was performed by silica gel chromatography, eluting with 90−100% EtOAc/hexanes. Fractions judged as containing product were pooled and solvent was evaporated, affording 64.2 mg (47%) of product. ^{1}H NMR (CD_3OD): δ 7.20 (m, 6H), 6.82 (d, 2H, J = 7 Hz), 4.81 (s, 4H), 3.96 (m, 2H), 3.99 (dd, 2H, J = 6.3, 6.5), 2.80 (s, 3H), 2.78 (s, 3H), 2.70 (m, 2H), 2.60 (t, 2H, J = 7.2), 1.57 (m, 2H), 1.34 (m, 9H). ^{13}C NMR (CD_3OD): δ 156.9, 129.9, 129.6, 124.1, 121.1, 121.0, 115.2, 80.6, 66.6, 59.6, 59.3, 56.4, 52.8, 52.12, 37.8, 37.6, 37.1, 32.4, 27.6, 25.2. ESMS: calculated *m*/*z* for $(MH)^+$ = 585.24, found = 585.15. HRMS: *m*/*z* calculated for $C_{26}H_{41}N_4O_7S_2$ $(MH)^+$ = 585.2407, found = 585.2413.

***tert*-Butyl 2-((4-(Methylsulfonamido)phenethyl)(2-(4-(methylsulfonamido)phenoxy)ethyl)amino)ethylcarbamate (7a).** The procedure is similar to the procedure for **7b**. ^{1}H NMR (CD_3OD): δ 7.29 (d, 2H, J = 8 Hz), 7.22 (m, 4H), 7.01 (d, 2H, J = 10 Hz), 4.37 (m, 2H), 3.77 (m, 2H), 3.52 (m, 6H), 3.09 (m, 2H), 2.92 (s, 3H), 2.87 (s, 3H), 1.48 (d, 9H). ESMS: calculated *m*/*z* for $(MH)^+$ = 571.23, found = 571.15. HRMS: *m*/*z* calculated for $C_{25}H_{39}N_4O_7S_2$ $(MH)^+$ = 571.2251, found = 571.2292.

***tert*-Butyl 6-((4-(Methylsulfonamido)phenethyl)(2-(4-(methylsulfonamido)phenoxy)ethyl)amino)hexylcarbamate (7e).** The procedure is similar to the procedure for **7b**. ^{1}H NMR (CD_3OD): δ 7.25 (d, 2H, J = 9hz), 7.23 (2d, 4H), 6.99 (d, 2H, J = 9 Hz), 4.36 (m, 2H), 3.71 (m, 2H), 3.46 (m, 2H), 3.30 (m, 2H), 3.07 (t, 2H), 3.01 (t, 2H), 2.92 (s, 3H), 2.88 (s, 3H), 1.78 (m, 2H), 1.47 (m, 6H), 1.40 (s, 9H). ^{13}C NMR (CD_3OD): δ 156.8, 139.0, 133.7, 133.4, 131.1, 125.2, 122.3, 116.6, 63.9, 56.2, 55.4, 53.6, 41.2, 39.4, 39.1, 30.9, 30.5, 28.9, 27.4, 27.3, 24.9. ESMS: calculated *m*/*z* for $(MH)^+$ = 627.29, found = 627.38. HRMS: *m*/*z* calculated for $C_{29}H_{47}N_4O_7S_2$ $(MH)^+$ = 627.2875, found = 627.2844.

***N*-[4-(2-{(3-Aminopropyl)[2-(4-methanesulfonylaminophenoxy)-ethyl]amino}ethyl)phenyl]methanesulfonamide, TFA Salt (9b).** An amount of 5.4 mg (9.2 μmol) of **7b** was dissolved in 2 mL of TFA. After 5 min, the solvent was evaporated. The resulting oil was rubbed with 25 mL of diethyl ether three times and then pumped on vacuum. The oil was analyzed by LC−ESMS, judged to be at least 95% pure, and then was used directly without further purification. ESMS: calculated *m*/*z* for $(MH)^+$ = 485.19, found = 485.14.

***N*-[4-(2-{(3-Aminoethyl)[2-(4-methanesulfonylaminophenoxy)-ethyl]amino}ethyl)phenyl]methanesulfonamide (9a), TFA Salt.** The procedure is similar to the procedure for **9b**. ESMS: calculated *m*/*z* for $(MH)^+$ = 471.17, found = 471.01.

***N*-[4-(2-{(3-Aminohexyl)[2-(4-methanesulfonylaminophenoxy)-ethyl]amino}ethyl)phenyl]methanesulfonamide (9e), TFA Salt.** The procedure is similar to the procedure for **9b**. ESMS: calculated *m*/*z* for $(MH)^+$ = 527.24, found = 527.51.

***N*-[4-(2-{[4-(1,3-Dioxo-1,3-dihydroisoindol-2-yl)butyl][2-(4-methanesulfonylaminophenoxy)ethyl]amino}ethyl)phenyl]-methanesulfonamide (8a), TFA Salt.** To a solution of 21 mg (50 μmol) of **2** in 2.0 mL of acetonitrile was added 5.0 mg (50 μmol) of Na_2CO_3 followed by 19 mg of *N*-(4-bromobutyl)phthalimide. The mixture was warmed to reflux. After 2 h, an additional 15 mg (53 μmol) of *N*-(4-bromobutyl)phthalimide was added. After an additional 2 h, the mixture was cooled to room temperature, 0.5 mL of ACN and 0.5 mL of water were added, and the product was isolated by purification via preparative C18 HPLC (10 mL/ min flow rate, 100% (0.1% TFA) water to 80% ACN 30 min). Collected fractions were analyzed by HPLC and appropriate fractions pooled and lyophilized. Yield = 16.6 mg (53%). ^{1}H NMR (CD_3OD): δ 7.81 (m, 4H), 7.27 (d, 2H, J = 9 Hz), 7.21 (m, 4H), 6.97 (d, 2H, J = 9 Hz), 4.36 (t, 2H, J = 5 Hz), 3.73 (m, 4H), 3.42 (m, 4H), 3.07 (m, 2H), 2.91 (s, 3H), 2.87 (s, 3H), 1.80 (m, 4H). ^{13}C NMR (CD_3OD): δ 168.8, 155.4, 137.6, 134.3, 132.4, 132.1, 129.7, 123.8, 123.0, 121.0, 115.4, 112.5, 62.6, 55.0, 53.6, 52.5, 38.1, 37.7, 36.5, 29.1, 25.5, 20.9. ESMS: calculated *m*/*z* for $(MH)^+$ = 629.21, found = 629.24. HRMS: *m*/*z* calculated for $C_{30}H_{37}N_4O_7S_2$ $(MH)^+$ = 629.2095, found = 629.2125.

***N*-[4-(2-{[4-(1,3-Dioxo-1,3-dihydroisoindol-2-yl)pentyl][2-(4-methanesulfonylaminophenoxy)ethyl]amino}ethyl)phenyl]-methanesulfonamide (8b), TFA Salt.** The procedure is similar to the procedure for **8a**. ^{1}H NMR (CD_3OD): δ 7.82 (m, 4H,), 7.28

(d, 2H, J = 9 Hz), 7.22 (m, 4H), 6.98 (d, 2H, J = 9 Hz), 4.37 (t, 2H, J = 5 Hz), 3.70 (m, 4H), 3.47 (m, 2H), 3.29 (m, 2H), 3.08 (m, 2H), 2.92 (s, 3H), 2.87 (s, 3H), 1.86 (m, 2H), 1.75 (m, 2H), 1.41 (m, 2H). ^{13}C NMR (CD_3OD): δ 168.8, 155.4, 137.6, 134.3, 132.4, 132.1, 129.7, 123.8, 122.9, 121.0, 115.3, 62.5, 58.7, 54.9, 53.8, 52.3, 38.1, 37.7, 36.8, 29.1, 27.7, 26.2, 23.4. ESMS: calculated *m/z* for $(MH)^+$ = 643.23, found = 643.27. HRMS: *m/z* calculated for $C_{31}H_{39}N_4O_7S_2$ $(MH)^+$ = 643.2251, found = 643.2421.

***N*-[4-(2-{(3-Aminopropyl)[2-(4-methanesulfonylaminophenoxy)-ethyl]amino}ethyl)phenyl]methanesulfonamide (9c), TFA Salt.** To a solution containing 6.3 mg (10 μmol) of **10c** dissolved in 500 μL of methanol was added 10 μL (310 μmol) of hydrazine. After 5 min at room temperature, the mixture was warmed to reflux for 2 h. The reaction was judged to be complete by HPLC, and the mixture was cooled to ambient temperature. The solution was purified by direct injection onto a preparative C18 HPLC column (as for **8a**). Collected fractions were analyzed by HPLC and appropriate fractions pooled and lyophilized. Yield = 2.9 mg (58%). ESMS: calculated *m/z* for $(MH)^+$ = 499.20, found = 498.97.

***N*-[4-(2-{(4-Aminobutyl)[2-(4-methanesulfonylaminophenoxy)-ethyl]amino}ethyl)phenyl]methanesulfonamide (9d), TFA Salt.** The procedure is similar to the procedure for **9c**. Yield = 58%. ESMS: calculated *m/z* for $(MH)^+$ = 513.22, found = 512.95.

Synthesis of 10e (Cy3B Conjugate of 9e), TFA Salt. To 5.0 mg (15.8 μmol) of Cy3B-NHS ester was added 1.0 mL of DMF followed by 50 μL of DIEA. The solution was added to 9.8 mg (15.8 μmol) of **9e**. After 5 min, the reaction was judged to be 85% complete by LC−ESMS. The reaction solution was directly purified by passage over a C18 preparative HPLC column as for **8a**. Collected fractions were analyzed by LC−ESMS, and appropriate fractions were pooled. Calculated product yield = 7.0 mg (86%). The solution was aliquoted and lyophilized to a powder. ^{1}H NMR (CD_3OD): δ 8.17 (s, 1H), 7.90 (s, 1H), 7.87 (d, 1H, J = 1hz), 7.43 (s, 1H), 7.36 (dd, 1H, J = 1 Hz, 8 Hz), 7.28 (m, 4H), 7.23 (m, 4H), 6.98 (d, 2H, J = 9 Hz), 4.67 (m, 2H), 4.37 (t, 2H), 4.34 (m, 1H), 3.91 (m, 1H), 3.71 (m, 1H), 3.33 (s,1H), 3.48 (m, 2H), 3.24 (m, 4H), 3.21 (m, 4H), 3.13 (m, 2H), 3.07 (m, 2H), 2.92 (s, 3H), 2.87 (s, 3H), 2.59 (m, 2H), 2.00 (m, 2H), 1.75 (m, 12H), 1.52 (m, 2H), 1.37 (m, 4H). ESMS: calculated *m/z* for $(MH)^+$ = 1069.4, found = 1068.9; calculated *m/z* for $(MH_2)^{+2}$ = 535.21, found = 535.14. HRMS: *m/z* calculated for $C_{55}H_{70}N_6O_{10}S_3$ $(MH_2)^{+2}$= 535.2150, found = 535.2267.

Synthesis of 10a (Cy3B Conjugate of 9a), TFA Salt. The procedure is similar to the procedure for **10e**. ESMS: calculated *m/z* for $(MH)^+$ = 1013.36, found = 1012.95; calculated *m/z* for $(MH_2)^{+2}$ = 507.19, found = 507.13.

Synthesis of 10b (Cy3B Conjugate of 9b), TFA Salt. The procedure is similar to the procedure for **10e**. ESMS: calculated *m/z* for $(MH_2)^{+2}$ = 514.19, found = 514.11. HRMS: *m/z* calculated for $C_{52}H_{64}N_6O_{10}S_3$ $(MH_2)^{+2}$= 514.1916, found = 514.2021.

Synthesis of 10c (Cy3B Conjugate of 9c), TFA Salt. The procedure is similar to the procedure for **10e**. ESMS: calculated *m/z* for $(MH_2)^{+2}$ = 521.20, found = 521.14.

Synthesis of 10d (Cy3B Conjugate of 9d), TFA Salt. The procedure is similar to the procedure for **10e**. ESMS: calculated *m/z* for $(MH_2)^{+2}$ = 528.21, found = 528.14.

Synthesis of [2-(6-{[2-(4-Methanesulfonylaminophenoxy)-ethyl][2-(4-methanesulfonylaminophenyl)ethyl]amino}-hexylcarbamoyl)ethyl]carbamic Acid *tert*-Butyl Ester (11a), TFA Salt. A solution of 4.9 mg (9.3 μmol) of **9e** in 100 μL of 10% DIEA in NMP was prepared. An amount of 10 μL of a 0.5 M solution containing 3-*tert*-butoxycarbonylaminopropionic acid (Boc-β-Ala-OH) was activated by HBTU and DIEA in stoichiometric amounts. After 5 min, an additional 5 μL was added. The reaction was judged by LC−ESMS to be approximately 75% complete. The reaction solution was directly purified by passage over a C18 preparative HPLC column as for **8a**. Collected fractions were analyzed by HPLC and appropriate fractions pooled and evaporated. Yield = 4.2 mg (65%). ESMS: calculated *m/z* for $(MH)^+$ = 698.33, found = 698.73.

Synthesis of *tert*-Butyl 6-(6-((4-(Methylsulfonamido)phenethyl)(2-(4-(methylsulfonamido)phenoxy)ethyl)amino)hexylamino)-6-oxohexylcarbamate (11b). The procedure is similar to the procedure for **11a**. ESMS: calculated *m/z* for $(MH)^+$ = 740.37, found = 740.78.

Synthesis of 12a (Cy3B Conjugate of Boc Deprotected 11a), TFA Salt. An amount of 3.5 mg (5.0 μmol) of compound **11a** was dissolved in 0.5 mL of TFA. After 2 min, the TFA was removed under a stream of nitrogen and placed under high vacuum for 3 h. The residue was dissolved in 400 μL of DMF and 100 μL of DIEA, and 5.0 mg (4.3 μmol) of Cy3B NHS ester was added. After 1 h at room temperature, the reaction mixture was directly purified by preparative C18 HPLC as for compound **8a**. Collected fractions were analyzed by HPLC and appropriate fractions pooled. Calculated product yield = 1.86 mg (23%). Pooled fractions were lyophilized to dryness. ESMS: calculated *m/z* for $(MH_2)^{+2}$ = 570.73, found = 570.67.

Synthesis of 12b (Cy3B Conjugate of Boc Deprotected 11b), TFA Salt. The procedure is similar to the procedure for **12a**. Calculated product yield = 1.67 mg (20%). ESMS $(MH_2)^{+2}$ *m/z* calculated = 591.76, found = 591.71.

Synthesis of 13 (the 5-Carboxyfluorescein Conjugate of 9e), TFA Salt. An amount of 7.1 mg (15 μmol) of 5-carboxyfluorescein NHS ester was mixed with 9.8 mg (16 μmol) of **9e** using the same conditions and methods as for **10e**. Yield = 4.32 mg (32%). ESMS: *m/z* calculated for $(MH)^+$ = 885.2, found = 885.33; *m/z* calculated for $(MH_2)^{+2}$ = 443.15, found = 443.09.

Synthesis of 14 (5-Carboxy TMR Conjugate of 9e), TFA Salt. An amount of 7.5 mg (14 μmol) of of 5-carboxy TMR NHS ester was mixed with 9.8 mg (16 μmol) of **9e** using the same conditions and methods as for **10e**. Yield = 2.2 mg (18%). ESMS: calculated *m/z* for MH^+ = 939.37, found = 939.46; calculated *m/z* for $(MH_2)^{+2}$ = 470.19, found = 470.14. HRMS: *m/z* calculated for $C_{49}H_{60}N_6O_9S_2$ $(MH_2)^{+2}$ = 470.1925, found = 470.2032.

Synthesis of 15 (Cy3B Ethylamide), TFA Salt. To 0.50 mg (0.15 μmol) of Cy3B NHS ester was added 100 μL of DMF followed by 0.50 mL of 2 M (1.0 mmol) ethylamine in methanol. After 10 min, the reaction was judged to be complete by LC−ESMS. The reaction solution was directly purified by passage over a preparative C18 HPLC column as for **8a**. Collected fractions were analyzed by LC−ESMS, and appropriate fractions were pooled and lyophilized. Calculated product yield = 0.22 mg (47%). ESMS: *m/z* calculated for $(MH)^+$ = 588.25, observed = 588.04.

Binding Assays. [^{3}H]Dofetilide scintillation proximity assays (SPA) were performed as previously described.[40] Fluorescence polarization (FP) binding assay methods are detailed in ref 21 and described briefly here. Membrane homogenates from HEK-293S (cell line no. 15-08) cells expressing the hERG product were prepared as follows. Cell pellets were thawed at room temperature and kept on ice. Buffer (50 mM Tris-HCl, 1 mM $MgCl_2$, 10 mM KCl, pH 7.4, at 4 °C) was added to each cell pellet (10 mL of buffer per 10 g of packed cell pellet), and the mixture was homogenized using an Omni LabTek homogenizer (20 000 rpm for 30 s). The homogenate was centrifuged at 48000*g* for 20 min at 3−5 °C in a Sorvall Evolution RC centrifuge and the supernatant discarded. The pellet was resuspended, homogenized (20 000 rpm for 10 s), and centrifuged as before. The resultant supernatant was discarded, and the final pellet was resuspended (100 mL of the above buffer per 10 g of packed cell pellet), homogenized (20 000 rpm for 10 s), dispensed in to tubes in 1.2 and 5 mL aliquots, and stored between −75 and −85 °C until use. Protein concentration was determined using a Coomassie Blue kit as per manufacturer's instructions (Sigma 610A and 610-11). Specific hERG protein levels of ≥10 pmol/mg total protein were required for FP assay. Membranes with <5 pmol/mg protein did not work in FP mode.

The Cy3B ligands **10e**, **12a**, and **12b** and MR121 ligand **6** were stored in 100% DMSO and diluted to 6 nM in assay buffer (50 mM Tris-HCl, 1 mM MgCl, 10 mM KCl, 0.05% Pluronic F127 (BASF, Mount Olive, NJ), pH 7.4, at 4 °C) on the day of the experiment. Test samples and controls were diluted in 6% DMSO and 0.05% Pluronic F127. Cell membranes were removed from

the −80 °C freezer and placed on ice after defrosting. When required, the defrosted membranes were homogenized using a polytronic device for no more than 10 s; they were then diluted in the above assay buffer to produce a working solution of 0.3 mg/mL. The assay was compiled by adding 10 μL of test compound or control solution, 10 μL of the Cy3B ligand, and 10 μL of cell membranes to a black 384-well plate (Matrix, catalog no. 4318). The plates were mixed and then incubated for a minimum of 2 h prior to reading on a Tecan Ultra (for Cy3B, excitation at 530 nm and emission at 590 nm; for MR121, excitation at 595 nm and emission at 680 nm). K_i values[22] were generated using Pfizer proprietary software.

Patch Clamp Electrophysiology. Testing was carried out in HEK293 cells transfected with the hERG gene[41] maintained at 37 °C in Minimum Essential Medium with Earle's salts and l-glutamine, 10% fetal bovine serum, 1 mM sodium pyruvate, 0.1 mM nonessential amino acids, and 0.4 mg/mL Geneticin. Membrane currents of cells continuously perfused with 35 °C extracellular recording saline (137 mM NaCl, 4 mM KCl, 1.8 mM $CaCl_2$, 1 mM $MgCl_2$, 10 mM HEPES, 10 mM D-glucose, pH 7.4, 335 mM mOs) were measured using whole-cell patch clamp[23] with a MultiClamp 700A amplifier (Molecular Devices) and 3−5 MΩ glass pipettes filled with intracellular recording saline (130 mM KCl, 1 mM $MgCl_2$, 10 mM HEPES, 5 mM Mg-ATP, 5 mM EGTA, pH 7.2, 320 mM mOs). The liquid junction potential was 4 mV, and access resistance was compensated by at least 80%. For characterization of ligand potency, the hERG channel current was activated with a voltage step to +20 mV for 1 s followed by a ramp to −80 mV at 0.5 V/s delivered at 0.25 Hz. Following 5 min of stable control recording in which rundown of the tail current peak was <2% per minute, ligand solution was continuously perfused into the recording chamber for evaluation of current blockade (10−25 min). Upon reaching an apparent steady state of current inhibition, cells were exposed to 1 μM **1** (dofetilide) to block any remaining channel current. The peak of the hERG channel tail current produced by the voltage ramp was plotted as a function of time. A linear regression of 5 min of control data prior to drug application was performed, and the linear fit of the control data was extrapolated for calculation of percent inhibition. Data were fit with the Hill equation in order to estimate IC_{50} values. To derive a time constant (τ) for onset of block, currents in the presence of compound were normalized to the rundown-corrected control current amplitude and plotted as a function of time and the decay phase was fit with a single-exponential equation. Time constants were compared using an ANOVA and Bonferroni procedure to control for multiple comparisons (a Bonferroni-corrected p value of <0.05 was considered significant).

Permeability Assays. Caco-2 cells were obtained from American Type Culture Collection (Rockville, MD). Cells were cultured at 37 °C with cell culture medium in an atmosphere of 10% CO_2 and 90% relative humidity. The cells were passaged upon reaching approximately 75−85% confluence from T-flasks using 0.05% trypsin−EDTA (Invitrogen, Gibco Laboratories, Grand Island, NY). Caco-2 cells were seeded in Transwells (Corning Costar, Cambridge, MA) at a density of 60 000 cells/cm^2. The cell culture medium was changed biweekly (every 72 h) and was changed 24 h prior to experimentation. Caco-2 cell monolayers were used for experimentation between 17 and 25 days after seeding. Caco-2 cell monolayers were preincubated for 30 min at 37 °C (temperature maintained throughout the experiment) with transport buffer containing 5 μM cyclosporin A. To begin transport experiments, donor solutions of test compound with 5 μM cyclosporin A were added to the donor compartment. For absorptive (apical (AP) to basolateral (BL)) transport, the AP compartment is the donor and the BL compartment is receiver. For secretory (from BL to AP) transport, the BL compartment is the donor and AL compartment is receiver. The appearance of test compound into receiver compartments was measured at 1 and 2 h. At the conclusion of the experiments, samples were taken from the donor compartments along with samples from the initial donor solutions and were saved for analysis. Cell monolayers on filters were exised, lysed with 70% ACN, and saved for analysis. Permeability assays were performed in triplicate. Caco-2 cell monolayer integrity was assessed immediately following transport experiments by determining the flux of 0.1 mg/mL Lucifer yellow over 1 h in the absorptive transport direction. Compounds were detected using quantitative HPLC−MS−MS.

The apparent permeability (P_{app}) was calculated using the equation

$$P_{app} = \frac{1}{(\text{area})(C_{D(0)})}\frac{dM_r}{dt}$$

where "area" is the surface area of the cell monolayer on the filter support (1.0 cm^2), $C_{D(0)}$ is the initial concentration of test compound applied to the donor chamber, t is time, M_r is the mass of compound appearing in the receiver compartment as a function of time, and dM_r/dt is the flux of the compound across the cell monolayer. The mass recovery of test compounds was assessed and found to be 86−117%.

Acknowledgment. The authors are grateful to Leonard Contillo for model compound synthesis, Navin Varshney for HRMS, Dr. John Soglia for expert mass spectral analyses, Rodger Pasieczny for patch clamp analysis, and Dr. C. Preston Hensley for helpful comments.

Supporting Information Available: Details of HPLC purity assessments for new compounds, table listing purity data, and HPLC chromatograms of **3**, **6**, and **10e**. This material is available free of charge via the Internet at http://pubs.acs.org.

References

(1) Spector, P. S.; Curran, M. E.; Keating, M. T.; Sanguinetti, M. C. Class III antiarrhythmic drugs block hERG, a human cardiac delayed rectifier K^+ channel: open-channel block by methanesulfonanilides. *Circ. Res.* **1996**, *78*, 499−503.

(2) Curran, M. E.; Splawski, I.; Timothy, K. W.; Vincent, G. M.; Green, E. D.; Keating, M. T. A molecular basis for cardiac arrhythmia: HERG mutations cause long QT syndrome. *Cell (Cambridge, Mass.)* **1995**, *80*, 795−803.

(3) Meadows, M. Why drugs get pulled off the market. *FDA Consum.* **2002**, *36* (1), 11−17.

(4) Snyders, D. J.; Chaudhary, A. High affinity open channel block by dofetilide of HERG expressed in a human cell line. *Mol. Pharmacol.* **1996**, *49*, 949−955.

(5) Kiehn, J.; Lacerda, A. E.; Wible, B.; Brown, A. M. Molecular physiology and pharmacology of HERG. Single-channel currents and block by dofetilide. *Circulation* **1996**, *94*, 2572−2579.

(6) Brown, A. M. hERG Assay, QT Liability, and sUdden Cardiac Death. In *Cardiac Safety of Noncardiac Drugs*; Morganroth, J., Gussak, I., Eds.; Humana Press: Totowa, NJ, 2005; pp 67−81.

(7) Dubin, A. E.; Nasser, N.; Rohrbacher, J.; Hermans, A. N.; Marrannes, R.; Grantham, C.; Van Rossem, K.; Cik, M.; Chaplan, S. R.; Gallacher, D.; Xu, J.; Guia, A.; Byrne, N. G.; Mathes, C. Identifying modulators of hERG channel activity using the PatchXpress planar patch clamp. *J. Biomol. Screening* **2005**, *10*, 168−181.

(8) Bridgland-Taylor, M. H.; Hargreaves, A. C.; Easter, A.; Orme, A.; Henthorn, D. C.; Ding, M.; Davis, A. M.; Small, B. G.; Heapy, C. G.; Abi-Gerges, N.; Persson, F.; Jacobson, I.; Sullivan, M.; Albertson, N.; Hammond, T. G.; Sullivan, E.; Valentin, J. P.; Pollard, C. E. Optimization and validation of a medium-throughput electrophysiology-based hERG assay using IonWorks HT. *J. Pharmacol. Toxicol. Methods* **2006**, *54*, 189−199.

(9) Finlayson, K.; Sharkey, J. A High-Throughput Binding Assay for HERG. In *Optimization in Drug Discovery. In Vitro Methods*; Zhengyin, Y., Caldwell, G. W., Eds.; Humana Press: Totowa, NJ, 2004; pp 353−368.

(10) Cheng, C. S.; Alderman, D.; Kwash, J.; Dessaint, J.; Patel, R.; Lescoe, M. K.; Kinrade, M. B.; Yu, W. A high-throughput HERG potassium channel function assay: an old assay with a new look. *Drug Dev. Ind. Pharm.* **2002**, *28*, 177−191.

(11) Chiu, P. J. S.; Marcoe, K. F.; Bounds, S. E.; Lin, C.-H.; Feng, J.-J.; Lin, A.; Cheng, F.-C.; Crumb, W. J.; Mitchell, R. Validation of a [^{3}H]astemizole binding assay in HEK293 cells expressing HERG K^+ channels. *J. Pharmacol. Sci. (Tokyo, Jpn)* **2004**, *95*, 311−319.

(12) Raab, C. E.; Butcher, J. W.; Connolly, T. M.; Karczewski, J.; Yu, N. X.; Staskiewicz, S. J.; Liverton, N.; Dean, D. C.; Melillo, D. G. Synthesis of the first sulfur-35-labeled hERG radioligand. *Bioorg. Med. Chem. Lett.* **2006**, *16*, 1692−1695.
(13) Dorn, A.; Hermann, F.; Ebneth, A.; Bothmann, H.; Trube, G.; Christensen, K.; Apfel, C. Evaluation of a high-throughput fluorescence assay method for hERG potassium channel inhibition. *J. Biomol. Screening* **2005**, *10*, 339−347.
(14) Berque-Bestel, I.; Soulier, J.-L.; Giner, M.; Rivail, L.; Langlois, M.; Sicsic, S. Synthesis and characterization of the first fluorescent antagonists for human 5-HT4 receptors. *J. Med. Chem.* **2003**, *46*, 2606−2620.
(15) Cha, J. H.; Zou, M.-F.; Adkins, E. M.; Rasmussen, S. G. F.; Loland, C. J.; Schoenenberger, B.; Gether, U.; Newman, A. H. Rhodamine-labeled 2b-carbomethoxy-3b-(3,4-dichlorophenyl)tropane analogues as high-affinity fluorescent probes for the dopamine transporter. *J. Med. Chem.* **2005**, *48*, 7513−7516.
(16) Tahtaoui, C.; Parrot, I.; Klotz, P.; Guillier, F.; Galzi, J.-L.; Hibert, M.; Ilien, B. Fluorescent pirenzepine derivatives as potential bitopic ligands of the human M1 muscarinic receptor. *J. Med. Chem.* **2004**, *47*, 4300−4315.
(17) Zaheer, A.; Wheat, T. E.; Frangioni, J. V. IRDye78 conjugates for near-infrared fluorescence imaging. *Mol. Imaging* **2002**, *1*, 354−364.
(18) Cross, P. E.; Arrowsmith, J. E.; Thomas, G. N.; Gwilt, M.; Burges, R. A.; Higgins, A. J. Selective class III antiarrhythmic agents. 1. Bis(arylalkyl)amines. *J. Med. Chem.* **1990**, *33*, 1151−1165.
(19) Diaz, G. J.; Daniell, K.; Leitza, S. T.; Martin, R. L.; Su, Z.; McDermott, J. S.; Cox, B. F.; Gintant, G. A. The [^{3}H]dofetilide binding assay is a predictive screening tool for hERG blockade and proarrhythmia: comparison of intact cell and membrane preparations and effects of altering [K^+]. *J. Pharmacol. Toxicol. Methods* **2004**, *50*, 187−199.
(20) Liu, H.; Ji, M.; Luo, X.; Shen, J.; Huang, X.; Hua, W.; Jiang, H.; Chen, K. New *p*-Methylsulfonamido phenylethylamine analogues as class III antiarrhythmic agents: design, synthesis, biological assay, and 3D-QSAR analysis. *J. Med. Chem.* **2002**, *45*, 2953−2969.
(21) Deacon, M.; Singleton, D.; Szalkai, N.; Pasieczny, R.; Peacock, C.; Price, D.; Boyd, J.; Boyd, H.; Steidl-Nichols, J.; Williams, C. Early evaluation of compound QT prolongation effects: a predictive 384-well fluorescence polarisation binding assay for measuring hERG blockade. *J. Pharmacol. Toxicol. Methods* **2007**, *55*, 238−247.
(22) Cheng, Y.-C.; Prusoff, W. H. Relation between the inhibition constant K1) and the concentration of inhibitor which causes fifty per cent inhibition (I50) of an enzymic reaction. *Biochem. Pharmacol.* **1973**, *22*, 3099−3108.
(23) Hamill, O. P.; Marty, A.; Neher, E.; Sakmann, B.; Sigworth, F. J. Improved patch-clamp techniques for high-resolution current recording from cells and cell-free membrane patches. *Eur. J. Physiol.* **1981**, *391*, 85−100.
(24) Veldkamp, M. W.; Van Ginneken, A. C. G.; Bouman, L. N. Single delayed rectifier channels in the membrane of rabbit ventricular myocytes. *Circ. Res.* **1993**, *72*, 865−878.
(25) Troutman, M. D.; Thakker, D. R. Novel experimental parameters to quantify the modulation of absorptive and secretory transport of compounds by P-glycoprotein in cell culture models of intestinal epithelium. *Pharm. Res.* **2003**, *20*, 1210−1224.
(26) Hamilton, G.; Cosentini, E. P.; Teleky, B.; Koperna, T.; Zacheri, J.; Riegler, M.; Feil, W.; Schiessel, R.; Wenzi, E. The multidrug-resistance modifiers verapamil, cyclosporine A and tamoxifen induce an intracellular acidification in colon carcinoma cell lines in vitro. *Anticancer Res.* **1993**, *13*, 2059−2063.
(27) Fiser, A.; Sali, A. MODELLER: generation and refinement of homology-based protein structure models. *Methods Enzymol.* **2003**, *374*, , 461−491 (*Macromolecular Crystallography, Part D*).
(28) Doyle, D. A.; Cabral, J. M.; Pfuetzner, R. A.; Kuo, A.; Gulbis, J. M.; Cohen, S. L.; Chait, B. T.; MacKinnon, R. The structure of the potassium channel: molecular basis of K^+ conduction and selectivity. *Science (Washington, D.C.)* **1998**, *280*, 69−77.
(29) Laskowski, R. A.; McArthur, M. W.; Moss, D. S.; Thornton, J. M. PROCHECK: A program to check the stereochemical quality of protein structures. *J. Appl. Crystallogr.* **1993**, *26*, 283−291.
(30) Lees-Miller, J. P.; Duan, Y.; Teng, G. Q.; Duff, H. J. Molecular determinant of high-affinity dofetilide binding to HERG1 expressed in Xenopus oocytes: involvement of S6 sites. *Mol. Pharmacol.* **2000**, *57*, 367−374.
(31) Jones, G.; Willett, P.; Glen, R. C.; Leach, A. R.; Taylor, R. Development and validation of a genetic algorithm for flexible docking. *J. Mol. Biol.* **1997**, *267*, 727−748.
(32) Zhang, J.-H.; Chung, T. D. Y.; Oldenburg, K. R. A Simple statistical parameter for use in evaluation and validation of high throughput screening assays. *J. Biomol. Screening* **1999**, *4*, 67−73.
(33) Perry, M.; De Groot, M. J.; Helliwell, R.; Leishman, D.; Tristani-Firouzi, M.; Sanguinetti, M. C.; Mitcheson, J. Structural determinants of HERG channel block by clofilium and ibutilide. *Mol. Pharmacol.* **2004**, *66*, 240−249.
(34) Perry, M.; Stansfeld, P. J.; Leaney, J.; Wood, C.; de Groot, M. J.; Leishman, D.; Sutcliffe, M. J.; Mitcheson, J. S. Drug binding interactions in the inner cavity of hERG channels: molecular insights from structure−activity relationships of clofilium and ibutilide analogs. *Mol. Pharmacol.* **2006**, *69*, 509−519.
(35) Pearlstein, R. A. V.; Roy, J.; Kang, J.; Chen, X.-L.; Preobrazhenskaya, M.; Shchekotikhin, A. E.; Korolev, A. M.; Lysenkova, L. N. M.; Olga, V.; Hendrixa, J.; Rampea, D. Characterization of HERG potassium channel inhibition using CoMSiA 3D QSAR and homology modeling approaches. *Bioorg. Med. Chem. Lett.* **2003**, *13*, 1829−1835.
(36) Rajamani, R.; Tounge, B. A.; Li, J.; Reynolds, C. H. A two-state homology model of the hERG K^+ channel: application to ligand binding. *Bioorg. Med. Chem. Lett.* **2005**, *15*, 1737−1741.
(37) Oesterberg, F.; Aqvist, J. Exploring blocker binding to a homology model of the open hERG K^+ channel using docking and molecular dynamics methods. *FEBS Lett.* **2005**, *579*, 2939−2944.
(38) Rajamani, R. T.; Brett, A.; Li, J.; Reynolds, C. H. A two-state homology model of the hERG K^+ channel: application to ligand binding. *Bioorg. Med. Chem. Lett.* **2005**, *15*, 1737−1741.
(39) More, J. D.; Finney, N. S. A simple and advantageous protocol for the oxidation of alcohols with *o*-iodoxybenzoic acid (IBX). *Org. Lett.* **2002**, *4*, 3001−3003.
(40) Greengrass, P. M.; Stewart, M.; Wood, C. M. Assay to establish the affinity of compounds at the ERG potassium channel, and use in identification of compounds with undesirable cardiac side effects. WO2003021271 A2, 2003.
(41) Zhou, Z.; Gong, Q.; Ye, B.; Fan, Z.; Makielski, J. C.; Robertson, G. A.; January, C. T. Properties of HERG channels stably expressed in HEK 293 cells studied at physiological temperature. *Biophys. J.* **1998**, *74*, 230−241.

JM0700565